*Control problems in nonlinear systems*

# Kinematic Navigation of a Mobile Robot to the Maximizer of an Environmental Field without Derivatives Estimation[1]

## A.S. Matveev,[1] M.C. Hoy, [2] and A.V. Savkin[3]

**[1] Department of Mathematics and Mechanics,
Saint Petersburg University,
Saint Petersburg, Russia,
[2,3] School of Electrical Engineering and Telecommunications,
the University of New South Wales,
Sydney, NSW, Australia
E-Mail: [1]almat1712@yahoo.com; [2]mch.hoy@gmail.com;
[3]a.savkin@unsw.edu.au**

### Abstract

We consider a single kinematically controlled mobile robot traveling in a planar region supporting an unknown field distribution. A single sensor provides the distribution value at the current robot location. We present a novel navigation strategy that drives the robot to the location where the field distribution attains its maximum. The proposed control algorithm employs estimation of neither the entire field gradient nor derivative-dependent quantities, like the rate at which the available measurement evolves over time, and is non-demanding with respect to both computation and motion. Its mathematically rigorous analysis and justification are provided. Simulation results confirm the applicability and performance of the proposed guidance approach.

**Keywords:** Navigation, Gradient Climbing, Source Seeking, Sliding mode control.

# 1   Introduction

The paper addresses the problem of driving a single robot to the maximizer of an unknown scalar environmental field. This may be thermal, magnetic, electric, or optical field, concentration of a chemical, physical, or biological agent, intensity of a spatial (electromagnetic, acoustic, etc.) signal, minus the distance to an unknown location, etc. Examples of missions where this problem is of interest include environmental studies, geological exploration, detecting and localizing the source of a hazardous chemicals leakage or vapor or radiation emission, sources of pollutants and plumes, hydrothermal vents, etc. This problem was studied under the names of source seeking/localizing [35, 29, 12] and gradient climbing/acsent [28, 7, 4, 8], though the both also admit wider meanings [9, 29, 2, 31, 14, 15, 32, 11, 16, 22, 6, 30, 24, 13, 21]. For source-seeking missions, the interest in maximizers is relevant if the field decays away from the source. Such situation is typical for steady sources and static environments, though even if it does not exactly hold, extremum seeking may be of sense for a primary advancement in a vicinity of the source, where alternative and more informed methods may be utilized to specify the source location. The name 'gradient climbing' highlights the dominant control paradigm: try to align the velocity vector of the robot with the field gradient. At the same time, this is a method of wide applicability, not confined to navigation towards extrema of environmental fields.

One of the basic challenges in seeking extrema of environmental fields arises from the fact that the field gradient is not directly measured in many typical scenarios. A good deal of extensive research in this area[2] was based on explicit on-line gradient estimation. This approach is especially beneficial for mobile sensor networks thanks to collaborative field measurements in many locations and data exchange [29, 28, 7, 4, 18]. However even in this scenario, data exchange degradation due to e.g., communication malfunctions and constraints may require each robot in the team to operate autonomously during a considerable time. The single robot scenario is much more challenging, unless many spatially distributed sensors are mounted on the robot to provide the field values at several essentially distant locations. However this may constitute a separate problem, like for micro and miniature robots. In any case, multiple vehicle/sensor scenario means more complicated and costly hardware.

A good deal of recent research in the area was devoted to the case where no

---

[2]We refer the reader to [28, 7, 12] for a survey.

multiple sensor information is available. Then a typical method to compensate for the lack of data is to get extra information via special 'exploration' maneuvers by systematically 'dithering' the sensor position around the basic path to the extremum, with subsequent non-model based gradient estimation [8, 35, 12]. For example, in accordance with a general approach to the wider problem of extremum-seeking design [3], the vehicle is excited with probing high-frequency sinusoidal [35, 12] or stochastic [25] inputs. A similar in spirit approach is extremum seeking by means of many robots performing biased random walks [27] or by two robots with access to relative positions of each other and rotational actuation [17]. However these methods rely, either implicitly or explicitly, on systematic side exploration maneuvers to collect rich enough data, which gives rise to serious concerns about waste of resources.

Neither intentional systematic exploration maneuvers nor gradient estimation were employed in the methods from [26, 5]. In [26], a sliding-mode navigation law was proposed that steers a single Dubins-car like mobile robot to the maximizer of an unknown field based on only a single-sensor and point-wise measurement of the field value. A PID controller fed by such measurement was presented in [5]. However, the proposed controllers numerically differentiate the sensor reading with respect to time, which gives rise to concerns about amplification of the measurement noises and its detrimental effects on the overall performance. Though these effects have been successfully avoided in the particular scenarios examined in [5, 26], the need to ensure this puts strong extra burden on controller parameters tuning since reliable numerical differentiation of sensor data is an intricate problem still representing a real challenge in practical setting [1, 33, 10]. In the case of [26], this is enhanced by the need to handle the potential threat of the so-called chattering [23], which cannot be ignored whenever sliding mode control is employed.

This paper presents a novel kinematic control paradigm for maximum seeking that is completely free from evaluation of any field-derivative data, uses only finite gains instead of sliding-mode control, and at the same time retains the benefits of the controller from [26], including monotonic, non-oscillatory convergence. Instead of conventionally trying to align the velocity vector with the gradient, it is proposed to keep the velocity orientation angle proportional to the discrepancy between the field value and a given linear ascending function of time. Mathematically rigorous justification of this control law is offered. We also describe a domain of the controller parameters for which the objective is achieved: the robot inevitably reaches the desired neighborhood of the

maximizer in a finite time and remains there afterwards. Convergence and performance of the proposed law, including non-oscillatory close-loop behavior, are confirmed by extensive computer simulations.

For complex dynamical systems, kinematic control is often the first step in controller design whose objective is to generate the velocity reference signal. The next step is to design a controller that tracks this signal by means of forces and torques. This two-stage design works well in many situations and is especially popular in the face of uncertainties in the dynamical loops. In this paper, we limit ourselves to only kinematic control and moreover, examine a non-restrictive holonomic model. At the same time, the proposed control law is such that it is directly applicable to non-holonomic Dubins-car like vehicles, provided that the vehicle's feasible turning rate conforms to the recommended control gains.

An algorithm somewhat similar to ours can be found in [5], which however uses the estimated time-derivative of the measurement. Another difference is that in [5], only a steady harmonic field was examined, which is a severe limitation, the performance during the transient and the behavior after reaching a vicinity of the maximizer were not addressed even for general harmonic fields, and the offered conditions for convergence were partly implicit by giving no explicit bound on some entities that were assumed sufficiently large. The focus of this paper is on generic fields (not necessarily harmonic), and we offer study of the entire maneuver with explicit conditions for non-local convergence.

The body of the paper is organized as follows. Section 2 presents the system, problem setup, and control law. The assumptions and main results are stated in Section 3. In Section 4, these results and the proposed controller design are illustrated for the simple yet instructive case of an isotropic distribution. All proofs are concentrated in Section 6 and Appendix. Section 5 is concerned with simulation results.

## 2 System description and problem setup

A planar point-wise robot travels in a two-dimensional workspace. The robot is controlled by the time-varying linear velocity $\vec{v}$ whose magnitude does not exceed a given constant $v$. The workspace hosts an unknown scalar field $D(\boldsymbol{r})$, where $\boldsymbol{r} := (x, y)^\top$ and $x, y$ are the absolute Cartesian coordinates in the plane $\mathbb{R}^2$. The objective is to drive the robot to the point $\boldsymbol{r}^0$ where $D(\boldsymbol{r})$ attains its maximum and then to keep it in a vicinity of $\boldsymbol{r}^0$, thus displaying the approximate

location of $\boldsymbol{r}^0$. The on-board control system has access only to the field value $d(t) := D[\boldsymbol{r}(t)]$ at the robot's current location $\boldsymbol{r}(t) = [x(t), y(t)]^\top$. No data about the derivatives of $D$ are available; in particular, the robot is aware of neither the gradient $\nabla D[\boldsymbol{r}(t)]$ nor the time-derivative $\dot{d}$ of the measurement $d$.

The kinematic model of the robot is as follows:

$$\dot{\boldsymbol{r}} = \vec{v}, \qquad \boldsymbol{r}(0) = \boldsymbol{r}_{\mathrm{in}} \qquad \|\vec{v}\| \leq v, \tag{1}$$

where $\|\cdot\|$ is the Euclidian norm. The problem is to design a controller that drives the robot into the $R_\star$-neighborhood of the maximizer $\boldsymbol{r}^0$

$$V_\star := \{\boldsymbol{r} : \|\boldsymbol{r} - \boldsymbol{r}^0\| \leq R_\star\} \tag{2}$$

in a finite time $t_0$ and then $t \geq t_0$ keeps the robot within $V_\star$.

In this paper, we propose and examine the following control algorithm:

$$\vec{v}(t) = v\vec{e}\left\{\mu\big[d(t) - v_*t\big] + \theta_0\right\}, \text{ where } \vec{e}(\theta) := \left(\begin{smallmatrix} \cos\theta \\ \sin\theta \end{smallmatrix}\right) \tag{3}$$

and $v_*, \mu > 0, \theta_0 \in \mathbb{R}$ are tunable parameters.

# 3   Assumptions and the main results

In general setting, the problem at hand comprises problems of global optimization, which are typically difficult to solve. In the presence of local extrema, NP-hardness, this mathematical seal for intractability, was established for even the simplest classes of such problems [20]. To avoid intractability, it is natural to assume absence of local extrema. So our first assumption considers a smooth field with a single global spatial maximizer $\boldsymbol{r}^0$ and no local extrema, which field converges to a finite limit $\gamma_{\mathrm{inf}}$ as $\|r\| \to \infty$.

**Assumption 1⁰** *The field $D(\cdot)$ is defined and $C^2$-smooth on the entire plane, there exists a point $\boldsymbol{r}^0$ such that $\nabla D(\boldsymbol{r}) \neq 0 \,\forall \boldsymbol{r} \neq \boldsymbol{r}^0$, and $\exists \lim_{\|\boldsymbol{r}\| \to \infty} D(\boldsymbol{r}) =: \gamma_{\mathrm{inf}} < D(\boldsymbol{r}^0)$.*

The reader satisfied by this postulation may proceed to Theorem 1. We however will in fact work with an essentially relaxed version of Assumption $1^0$. The relaxation takes into account that $D(\cdot)$ often results from an interplay of a basic field and perturbations, and the latter are likely to cause local extrema in the regions where the basic field is flat enough. By the Fermat theorem, one such region surrounds the maximizer. For most physical fields, another region

lies far enough from the maximizer, where the energy of the basic field becomes distributed over large areas.

In view of this, we assume that the plane is partitioned into a 'vicinity' of the maximizer $Z_{\text{near}}$, outskirts $Z_{\text{far}}$, and an intermediary $Z_{\text{reg}}$. In $Z_{\text{near}} \cup Z_{\text{far}}$, the field $D(\cdot)$ is more or less arbitrary, may have local maxima or even be non-smooth. In $Z_{\text{reg}}$, the field is smooth and has no critical points and thus local extrema. To reduce technicalities, we also assume that these zones are separated by isolines $I(\gamma) := \{ \boldsymbol{r} : D(\boldsymbol{r}) = \gamma \}$, which can usually be achieved by properly reducing $Z_{\text{reg}}$. On $Z_{\text{near}}$, the field $D(\cdot)$ is assumed to take greater values than on the complement. So the maximizer belongs to $Z_{\text{near}}$, which justifies the above interpretation of $Z_{\text{near}}$.

Summarizing, we arrive at the following.

**Assumption 1** *There exist $\gamma_- < \gamma_+$ such that on $Z_{reg} := \{ \boldsymbol{r} : \gamma_- \leq D(\boldsymbol{r}) \leq \gamma_+ \}$, the distribution $D(\cdot)$ is identical to a $C^2$-smooth function defined on a larger and open set, $\nabla D(\boldsymbol{r}) \neq 0 \ \forall \boldsymbol{r} \in Z_{reg}$, the isoline $I(\gamma_-)$ is a Jordan curve and encircles $I(\gamma_+)$. Inside $I(\gamma_+)$, the field $D(\cdot)$ is defined and continuous everywhere, maybe except for finitely many points $\boldsymbol{r}_*$ where $\lim_{\boldsymbol{r} \to \boldsymbol{r}_*} D(\boldsymbol{r}) = \infty$, and takes values greater than $\gamma_+$. Inside $I(\gamma_-)$, the field is defined everywhere, is continuous, and takes values lesser than $\gamma_-$.*

Exceptional points $\boldsymbol{r}_*$ occur only for some theoretical distributions, like $D(\boldsymbol{r}) = c/\|\boldsymbol{r} - \boldsymbol{r}^0\|$ or $D(\boldsymbol{r}) = -c \ln \|\boldsymbol{r} - \boldsymbol{r}^0\|$; these points are viewed as furnishing the infinite maximum. Modulo this, Assumption 1 implies that $\sup_{\boldsymbol{r} \in \mathbb{R}^2} D(\boldsymbol{r})$ is attained at some point $\boldsymbol{r}^0$. If there are several maxima, the control objective should be achieved for one of them.

**Assumption 2** *For some maximizer $\boldsymbol{r}^0$, the isoline $I(\gamma_+)$ lies in the interior of the vicinity (2). The initial location lies in the domain of $D(\cdot)$ and inside $I(\gamma_-)$, i.e., $\gamma_- < D(\boldsymbol{r}_{in})$.*

**Remark 1** Suppose that Assumption $1^0$ holds. Then so evidently does Assumptions 1, where $\gamma_\pm$ can be arbitrarily chosen subject to $\gamma_{\text{inf}} < \gamma_- < \gamma_+ < D(\boldsymbol{r}^0)$. As $\gamma_- \to \gamma_{\text{inf}}$ and $\gamma_+ \to D(\boldsymbol{r}^0)$, the set $Z_{\text{reg}}$ covers any given annulus $\{ \boldsymbol{r} : 0 < \varepsilon < \|\boldsymbol{r} - \boldsymbol{r}^0\| < R < \infty \}$. It follows that Assumption 2 is valid as well.

The first theorem shows that the control objective can always be achieved by means of the control law (3).

**Theorem 1** *Suppose that either Assumption $1^0$ or Assumptions 1 and 2 hold. Then there exist parameters $v_*, \mu, \theta_0$ of the controller (3) such that the following statement is true:*

(i) *The controller (3) brings the robot to the desired vicinity (2) of a maximizer in a finite time $t_0$ and subsequently keeps it there: $\boldsymbol{r}(t) \in V_\star \; \forall t \geq t_0$.*

*Moreover, for any compact domain $D \subset \mathbf{int} Z_{reg}$, there exist common values of the parameters for which* (i) *holds whenever the initial location $\boldsymbol{r}_{in} \in D$.*

The proofs of the results stated in this section will be given in Sect. 6.
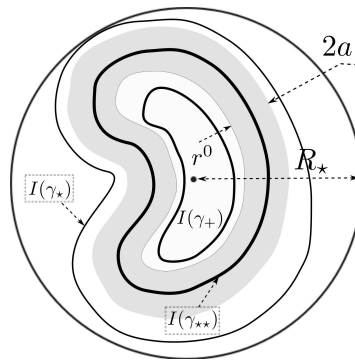


Figure 1: Two isolines

In the rest of the section, we discuss controller tuning. It is orchestrated by two auxiliary parameters $\gamma_{\star\star} \in (\gamma_\star, \gamma_+)$ and $a > 0$. Here

$$\gamma_\star := \max_{\boldsymbol{r} : \|\boldsymbol{r} - \boldsymbol{r}^0\| = R_\star} D(\boldsymbol{r}) < \gamma_+. \tag{4}$$

and $a$ is chosen so that (see Fig. 1)

$$0 < a < \mathbf{dist}\left[I(\gamma_\star); I(\gamma_{\star\star})\right], a < \mathbf{dist}\left[I(\gamma_{\star\star}); I(\gamma_+)\right],$$
$$\text{and } a < \mathbf{dist}\left[I(\gamma_-); I[D(\boldsymbol{r}_{in})]\right] \text{ if } D(\boldsymbol{r}_{in}) < \gamma_{\star\star}. \tag{5}$$

Here $\mathbf{dist}\,[A; B] := \inf_{\boldsymbol{r}_a \in A, \boldsymbol{r}_b \in B} \|r_a - r_b\|$ is the distance between the sets $A$ and $B$. We also introduce the set:

$$W(a, \gamma_{\star\star}) := \{\boldsymbol{r} : \gamma_{in} \leq D(r) \leq \gamma_{\star\star}\}, \tag{6}$$
$$\text{where} \quad \gamma_{in} := \min_{\boldsymbol{r} : \mathbf{dist}(\boldsymbol{r}; I[D(\boldsymbol{r}_{in})]) \leq a \text{ or } \|\boldsymbol{r} - \boldsymbol{r}^0\| = R_\star} D(\boldsymbol{r}).$$

Due to Assumption 1, this set is compact since $\gamma_{in} > \gamma_-$.

The parameters $\theta_0, v_*$ of the controller (3) are chosen prior to $\mu$. Whereas $\theta_0$ is arbitrary, $v_*$ is such that

$$0 < v_*/v < \Xi := \min_{\boldsymbol{r} \in W(a, \gamma_{\star\star})} \|\nabla D(\boldsymbol{r})\|. \tag{7}$$

To tune $\mu$, we use some functions that characterize the gradient $\nabla D(\boldsymbol{r})$ rate of change with respect to $\boldsymbol{r}$. For $\boldsymbol{r} \neq \boldsymbol{r}^0, \alpha \in (-\pi/2, \pi/2)$, we put

$$\varkappa(\alpha, \boldsymbol{r}) := \frac{\left\langle D''(\boldsymbol{r})\Phi_{\frac{\pi}{2}-\alpha}\nabla D(\boldsymbol{r}); \Phi_{\frac{\pi}{2}-\alpha}\nabla D(\boldsymbol{r})\right\rangle}{\cos\alpha\|\nabla D(\boldsymbol{r})\|^3}, \tag{8}$$

where $\Phi_\alpha$ is the matrix of rotation through angle $\alpha$:

$$\Phi_\alpha := \begin{pmatrix} \cos\alpha & -\sin\alpha \\ \sin\alpha & \cos\alpha \end{pmatrix}. \tag{9}$$

Here $\varkappa(0, \boldsymbol{r})$ is the signed curvature of the isoline $I := \{\boldsymbol{r}' : D(\boldsymbol{r}') = D(\boldsymbol{r})\}$ at the point $\boldsymbol{r}$. For $\alpha \neq 0$, the following remark is illuminative; its proof is given in Appendix A.

**Remark 2** In any simply connected open domain $D \not\ni \boldsymbol{r}^0$, the gradient can be represented in the form $\nabla D(\boldsymbol{r}) = \rho(\boldsymbol{r})\vec{e}[\varphi(\boldsymbol{r})]$, where $\rho(\boldsymbol{r}) := \|\nabla D(\boldsymbol{r})\|$ and the angle of the gradient orientation $\varphi(\cdot)$ is $C^2$-smooth. In these terms,

$$\varkappa(\alpha, \boldsymbol{r}) = \left\langle \nabla\varphi; \Phi_{\frac{\pi}{2}-\alpha}\vec{e}[\varphi]\right\rangle + \tan\alpha \left\langle \nabla\varphi; \vec{e}(\varphi)\right\rangle -$$
$$\frac{2\ln 10}{10}\tan\alpha \sin\frac{\alpha}{2} \left\langle \nabla\left(10\log_{10}\rho\right); \Phi_{-\frac{\alpha}{2}}\vec{e}[\varphi]\right\rangle, \tag{10}$$

where the values of all functions are taken at $\boldsymbol{r}$.

Formula (10) is arranged so that for small $\alpha$, the order of the addend ascends from the beginning to the end. In (10),

a) the first addend is the curvature of the curve that transverses the gradient vector field at the constant angle $\frac{\pi}{2} - \alpha$ (or equivalently, transverses the isolines at the angle $-\alpha$);

b) the multiplier $\left\langle \nabla\varphi; \vec{e}(\varphi)\right\rangle$ in the second addend is the curvature of the curve that goes in the gradient direction;

c) the multiplier $\left\langle \nabla\left(10\log_{10}\rho\right); \Phi_{-\frac{\alpha}{2}}\vec{e}[\varphi]\right\rangle$ in the last addend is the rate at which the gradient intensity $\|\nabla D\|$ (measured in Db) changes along the curves that transverse the gradient vector field at the constant angle $-\frac{\alpha}{2}$.

The next function characterizes not the rate but the overall change of the gradient direction as $\boldsymbol{r}$ goes not necessarily in special directions. For any closed disc $\mathfrak{D} \not\ni \boldsymbol{r}^0$, the angle $\beta$ of rotation of the vector-field $\nabla D$ along a curve $\mathfrak{D} \subset Z_{\text{reg}}$ is uniquely determined by the ordered pair of the ends of $\gamma$ since $\nabla D(\boldsymbol{r}) \neq 0 \; \forall \boldsymbol{r} \in \mathfrak{D}$ by Assumption 2. Let $\beta(\mathfrak{D})$ be the maximum of $|\beta|$ over all pairs in $\mathfrak{D}$. We put

$$B(a) := \max_{\mathfrak{D}} \beta(\mathfrak{D}), \tag{11}$$

where the maximum is over all disks of the radius $a$ centered either at $\boldsymbol{r}_{\text{in}}$ or on $I(\gamma_{\star\star})$.

The choice of the parameter $\mu$ is subjected to the constraint

$$\mu > v \min_{\delta \leq v_*, v\Xi - v_*} \frac{\lambda(\delta, a)}{\delta}, \qquad \text{where} \quad \lambda(\delta, a) := \tag{12}$$

$$\max \left\{ \max_{\substack{\boldsymbol{r} \in W(a, \gamma_{\star\star}) \\ |\alpha| \leq \alpha(v_* + \delta, \boldsymbol{r})}} |\varkappa(\alpha, \boldsymbol{r})| \, ; \, \frac{2}{a} \left( \left\lceil \frac{B(a)}{2\pi} \right\rceil + 1 \right) \right\},$$

$$\alpha(\delta, \boldsymbol{r}) := \arcsin \frac{\delta}{v \|\nabla D(\boldsymbol{r})\|}, \tag{13}$$

$\Xi$ is given by (7), and $\lceil z \rceil$ is the integer ceiling of $z$. This formula shows how 'large' $\mu$ should be in the last paragraph from Sect. 2.

**Theorem 2** *Suppose that the assumptions of Theorem 1 hold and for some a obeying (5), the controller parameters satisfy (7) and (12). Then* (i) *from Theorem 1 is true.*

**Remark 3**    i) Consecutive choice of the parameters satisfying (5), (7), and (12) is always possible since the right-hand sides of the inequalities from (5) and (7) are positive, whereas the right-hand side of (12) is finite.

   ii) Practically, this choice is typically based on estimates of the domain $W(a, \gamma_{\star\star})$ and the concerned characteristics of $D(\cdot)$ based on an a priory knowledge about the field.

iii) Now we outline a way to follow these lines in the case from Remark 1, assuming that $D[\boldsymbol{r}_{\text{in}}] < \min_{\boldsymbol{r}: \|\boldsymbol{r} - \boldsymbol{r}^0\| = R_\star} D(r)$ to reduce technicalities. The starting step is upper estimating the isoline $I[D(\boldsymbol{r}_{\text{in}})]) \subset \mathbf{int}C$ by a compact simply connected domain $C \supset \{\boldsymbol{r} : \|\boldsymbol{r} - \boldsymbol{r}^0\| \leq R_\star\}$, and lower estimating the distances from (5), where $I(\gamma_-)$ and $I(\gamma_+)$ are replaced by

the boundary of $C$ and $\{r^0\}$, respectively, in accordance with the last claim from Remark 1. Let $\nu(\gamma_{\star\star})$ be the minimum among these estimates. It is reasonable to pick $\gamma_{\star\star}$ as the maximizer $\gamma_0$ of $\nu(\cdot)$. Then $W(a, \gamma_{\star\star}) \subset \widehat{W} := \{r \in C : \|r - r^0\| \geq \nu(\gamma_0)\}$. Hence the last inequality from (7) is implied by

$$v_*/v < \widehat{\Xi} := \min_{r \in \widehat{W}} \|\nabla D(r)\|.$$

This is constructive if a lower estimate of the gradient is available, whereas the other inequalities regulating the choice of $v, v_*$ are explicit. As for $\mu$, we put $q(r) := \frac{\|D''(r)\|}{\|\nabla D(r)\|}$ and note that by (11), $|B(a)| \leq 2a\zeta(a)$, where

$$\zeta(a) := \max_{r \in \widehat{W} \text{ or } \nu(\gamma_0) - a \leq \|r - r^0\| \leq \nu(\gamma^0)} \frac{\|D''(r)\|}{\|\nabla D(r)\|}.$$

Since the first argument in the max from (12) is not affected by $a$ and the second does not exceed $\Omega(a) := 4(\frac{\zeta(a)}{2\pi} + \frac{1}{a})$, it is reasonable to pick $a$ so that it nearly furnishes $\inf_{a \in (0, \nu(\gamma_0))} \Omega(a)$. Furthermore, in (12),

$$\max_{\substack{r \in W(a, \gamma_{\star\star}) \\ |\alpha| \leq \alpha(v_* + \delta, r)}} |\varkappa(\alpha, r)|$$

$$\overset{(8)}{\leq} \max_{r \in \widehat{W}} \max_{|\alpha| \leq \alpha(v_* + \delta, r)} \frac{\|D''(r)\|}{\|\nabla D(r)\| \cos \alpha}$$

$$\overset{(13)}{=} \max_{r \in \widehat{W}} \frac{v \|D''(r)\|}{\sqrt{\|\nabla D(r)\|^2 - \frac{(v_* + \delta)^2}{v^2}}}$$

$$\leq \frac{v \max_{r \in \widehat{W}} \|D''(r)\|}{\sqrt{\widehat{\Xi}^2 - \frac{(v_* + \delta)^2}{v^2}}}.$$

Thus we see that the requirement (12) to $\mu$ is implied by

$$\mu > v \min_{\delta \leq v_*, v\widehat{\Xi} - v_*} \max \left\{ \frac{vQ}{\delta \sqrt{\widehat{\Xi}^2 - \frac{(v_* + \delta)^2}{v^2}}} ; \frac{\Omega(a)}{\delta} \right\},$$

which is constructive whenever an upper estimate $Q \geq \|D''(r)\| \; \forall r \in \widehat{W}$ of the second derivative is available.

The estimates underlying iii) are essentially rough; relatively brief presentation is the main reason to discuss this method. More sophisticated approaches based on extra a priory knowledge are illustrated in the next section.

# 4  Isotropic Distribution

Now we illustrate the discussion of the previous section in the simple yet instructive case where the scalar field is caused by energy emanation from a point-wise source, and we deal with this process at equilibrium. In isotropic media, the mathematical model for such fields is often as follows:

$$D(\boldsymbol{r}) = cf(\|\boldsymbol{r} - \boldsymbol{r}^0\|), \tag{14}$$

where $c$ characterizes the energy of the source and is unknown, whereas the twice continuously differentiable function $f : (0, \infty) \to \mathbb{R}$ is known, strictly decaying and convex

$$f'(z) < 0, \qquad f''(z) > 0 \qquad \forall z > 0, \tag{15}$$

with $f(z) := \frac{1}{z}$ and $f(z) := -\ln z$ being typical examples. The location $\boldsymbol{r}^0$ of the source is unknown. The objective is to display this location by bringing the robot to its vicinity (2) on the basis of the following known estimates

$$c \geq c_- > 0, \qquad \left\| \boldsymbol{r}_{\text{in}} - \boldsymbol{r}^0 \right\| \leq R_{\text{in}}. \tag{16}$$

We assume that $R_{\text{in}} > R_\star$ to simplify the formulas.

**Corollary 1** *Suppose that* (14)—(16) *hold and the parameters of the controller* (3) *are chosen so that*

$$0 < v_*/v < \Xi_* := c_-|f'(R_{\text{in}} + R_\star/2)|, \tag{17}$$

$$\mu > v \min_{\substack{\delta \leq v_* \\ v\Xi_* - v_*}} \max \left\{ \frac{8}{\delta R_\star} \, ; \, \max_{R_\star/2 \leq z \leq R_{\text{in}} + R_\star/2} B(z, \delta) \right\}$$

$$B(z, \delta) := \left[ \frac{1}{\delta z} + \frac{\delta f''(z)}{v c_- f'(z)^2 \sqrt{c_-^2 v^2 f'(z)^2 - \delta^2}} \right]. \tag{18}$$

*Then the robot driven by the controller* (3) *reaches the desired vicinity* (2) *of the maximizer in a finite time and remains there afterwards.*

In the typical cases where $f(z) = \frac{1}{z}$ or $f(z) = -\ln z$, elementary calculus show that $B(z, \delta)$ is convex with respect to $z$ and so attains its maximum over $z \in [R_\star/2, R_{\text{in}} + R_\star/2]$ at the ends of the interval. Thus (18) shapes into

$$\mu > v \min_{\substack{\delta \leq v_* \\ v\Xi_* - v_*}} \max \left\{ \frac{8}{\delta R_\star} \, ; B(R_\star/2, \delta) \, ; B(R_{\text{in}} + R_\star/2, \delta) \right\}$$

and for particular $v_* := \lambda v \Xi_*, \lambda \geq 1/2$ is implied by

$$\mu > v \max \left\{ \frac{8}{R_\star(1-\lambda)v\Xi_*} \, ; \, B(R_\star/2, (1-\lambda)v\Xi_*) \, ; \right.$$

$$\left. B(R_{\text{in}} + R_\star/2, (1-\lambda)v\Xi_*) \right\}.$$

**PROOF OF COROLLARY 1:** Assumption 1 holds with $\gamma_- \approx 0$ and $\gamma_+ \approx \infty$ since

$$\nabla D(\boldsymbol{r}) = cf'(\|\boldsymbol{r} - \boldsymbol{r}^0\|)\frac{\boldsymbol{r} - \boldsymbol{r}^0}{\|\boldsymbol{r} - \boldsymbol{r}^0\|} \neq 0 \forall \boldsymbol{r} \neq \boldsymbol{r}^0. \tag{19}$$

The isolines are circles centered at $\boldsymbol{r}^0$. In (5), $I(\gamma_{\star\star})$ can have any radius $R_{\star\star} \in (0, R_\star)$ modulo the freedom to manipulate $\gamma_{\star\star}$ and $\gamma_+$, and $0 < a < \min\{R_\star - R_{\star\star}; R_{\star\star}\}$. For $R_{\star\star} := R_\star/2, a := R_\star/2 - \varepsilon, \varepsilon > 0, \varepsilon \approx 0$, (6) yields

$$W(a, \gamma_{\star\star}) \subset \left\{ \boldsymbol{r} : R_{\star\star} \leq \|\boldsymbol{r} - \boldsymbol{r}^0\| \leq R_{\text{in}} + \frac{R_\star}{2} \right\}. \tag{20}$$

So (7) follows from (16) and (19) (for small enough $\varepsilon$). As for (12), we note that for the radial vector-field (19) (see Fig. 2(a)), the maximal directional divergence $\beta(\mathfrak{D})$ from (11) is achieved at the points $\boldsymbol{r}_-, \boldsymbol{r}_+$ from Fig. 2(b) and so $\beta(\mathfrak{D}) = 2\arcsin\frac{a}{\|\boldsymbol{r}_* - \boldsymbol{r}^0\|}$. Hence by (11), $B(a) = 2\arcsin\frac{a}{R_{\star\star}-a} < \pi$ and in (12),
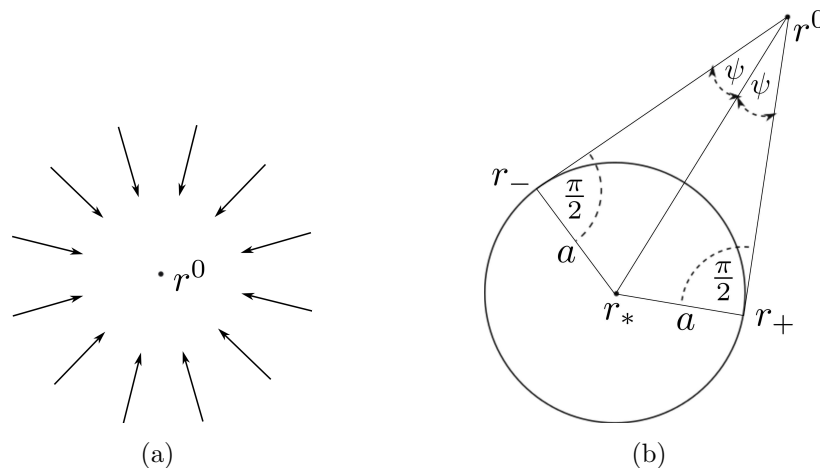


Figure 2: (a) Radial vector-field, (b) Maximal directional divergence

$\frac{2}{a}\left(\left\lceil \frac{B(a)}{2\pi} \right\rceil + 1\right) = \frac{8}{R_\star}$. To evaluate $\varkappa(\alpha, \boldsymbol{r})$, we separately estimate the addends in (10). For the radial vector-field (19), the curve from claim a) (following Remark 2) is the equiangular spiral. At a given point $\boldsymbol{r}$, the maximal among such spirals curvature is achieved in the case where the angle between the curve tangent and the radial line is right [19], i.e., for the circle. Hence the modulus

of the first addend in (10) does not exceed $\|\boldsymbol{r} - \boldsymbol{r}^0\|^{-1}$. The second addend is zero since the curves from b) are radial straight lines. Since the gradient from the third addend is evidently radial (see Fig. 2(a)), this addend is equal to $2 \tan \alpha \sin \frac{\alpha}{2} \frac{f''(\|\boldsymbol{r}-\boldsymbol{r}^0\|)}{f'(\|\boldsymbol{r}-\boldsymbol{r}^0\|)} \cos \frac{\alpha}{2}$. Thus

$$|\varkappa(\alpha, \boldsymbol{r})| \leq \|\boldsymbol{r} - \boldsymbol{r}^0\|^{-1} + |\tan \alpha||\sin \alpha| \frac{|f''(\|\boldsymbol{r} - \boldsymbol{r}^0\|)|}{|f'(\|\boldsymbol{r} - \boldsymbol{r}^0\|)|}$$

and so (12) follows from (18) and (20). Theorem 2 completes the proof.  □

## 5   Results of the Simulation Tests

Simulations were carried out with the point-mass robot (1) driven by the control law (3). The numerical values of the parameters used for simulations are shown in Table 1 (where $u_d$ is the unit of measurement of the field value $d = D(\boldsymbol{r})$). The control was updated with a sampling time of $0.1s$.

| $v$ | $1m/s$ | $\mu$ | $0.8rad/u_d$ |
|-----|--------|-------|--------------|
| $v_*$ | $0.299u_d/s$ | $\theta_0$ | $1.5rad$ |

Table 1: Numerical values of the parameters used for simulation.

The first test deals with the linear field

$$D(x, y) = n\big(x \cos \varphi + y \sin \varphi\big) + D_0,$$

where $n > 0, \varphi, D_0 \in \mathbb{R}$ are given. Since any smooth field is well approximated by a linear one in sufficiently small (and sometimes not so small) areas, the focus on linear fields permits us to disclose basic behavioral primitives that underly, more or less, the closed-loop behavior in general fields. A typical simulation result is displayed in Fig. 3 for the field with the orientation angle of 0.5 rad and the ascension rate of $0.3m^{-1}$. It demonstrates monotonic, non-oscillatory gradient climbing with the steady state angular error of $\approx 0.082rad$.

Fig. 4 presents the results of tests in the following field with a point-wise source:

$$D(\boldsymbol{r}) = -0.8 \cdot \|\boldsymbol{r} - \boldsymbol{r}^0\|.$$

As can be seen, the robot succesfully converges to the source and then wheels around it in a close proximity, thus displaying its location.

(a)



(b)
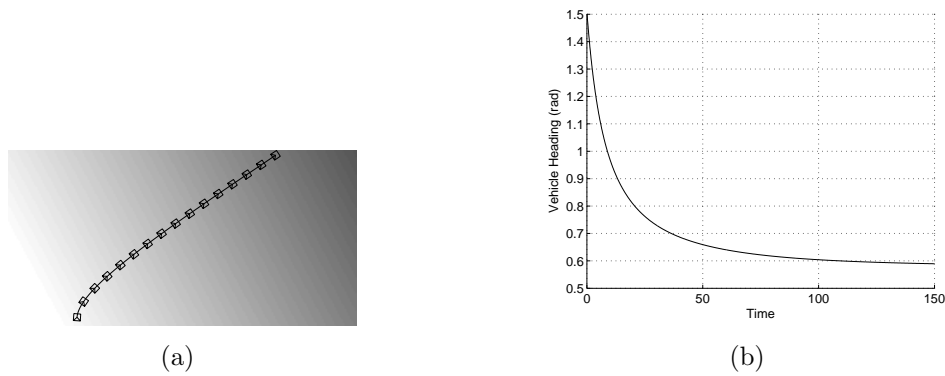
Figure 3: Behavior in a linear field: (a) Path (b) Robot's orientation



(a)



(b)
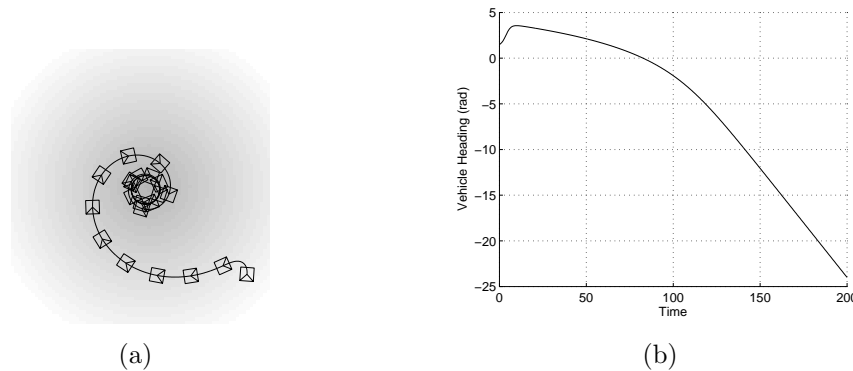
Figure 4: Seeking a point source: (a) Path (b) Robot's orientation

In Fig. 5, the same simulation setup was used, except measurement noise, a different field shape, and kinematic constraints were added. The robot's heading was not allowed to change faster than $0.5 rads^{-1}$, which in fact transforms (1) into the non-holonomic Dubins-car model since the robot's speed is constant by (3). The field readings were corrupted by a random additive noise uniformly distributed over the interval $[-2.5, 2.5]$, whereas the field was corrupted by two perpendicular plane waves:

$$D(\boldsymbol{r}) = -0.8 \cdot \|\boldsymbol{r} - \boldsymbol{r}^0\| + 5 \cdot [\sin(0.05 \cdot x) + \sin(0.05 \cdot y)].$$

However all these do not essentially alter the closed-loop behavior.

Fig. 6 is concerned with even more intricate scenario where in the simulation setup from Fig. 5, the field source moves from left to right. As can be seen, the vehicle still successfully reaches the source and then escorts it in a close proximity.

Simulations were also carried out for a more realistic model of a field caused by a constant-rate emanation of a certain substance (heat, gas, etc.) from a point-wise source and its subsequent steady state diffusion in an isotropic two-
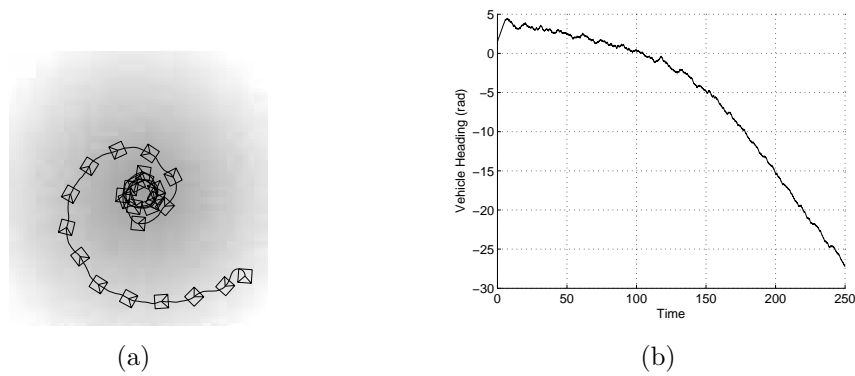
Figure 5: Seeking a source under measurement noise and kinematic constraints: (a) Path (b) Robot's orientation
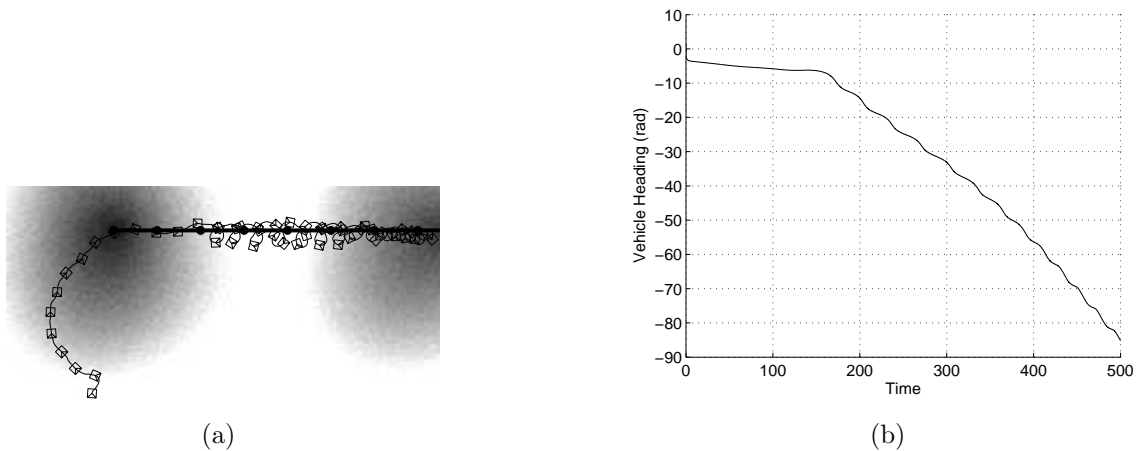


Figure 6: Simulations with a moving source.

dimensional medium. In many cases, this process is described by the heat equation $\partial D/\partial t = \rho \Delta D + \delta[\boldsymbol{r} - \boldsymbol{r}^0(t)]$. Here $\Delta$ is the spatial Laplacian, $\rho = 16000 m^2 s^{-1}$ is the diffusion rate, $\delta$ is the spatial Dirac delta-function, $\boldsymbol{r}^0(t)$ is the source location, and the emanation rate was set to unity. The steady state field distribution was calculated prior to navigation tests by the finite difference method. In doing so, the time and space steps were $0.001 s$ and $4m$, respectively. To approximately generate to steady state distribution, the system was simulated for $100 s$. and only then commenced motion the results were stored with the sampling rate $1 s$. During the navigation test, the distribution value was obtained through bilinear interpolation over each spatial step. Like in the previous experiment, the vehicle turning rate was bounded by $0.5 rads^{-1}$.

The results of these simulations are shown in Figs. 7. It may be seen in all cases the correct behavior was observed.

(a)                                             (b)
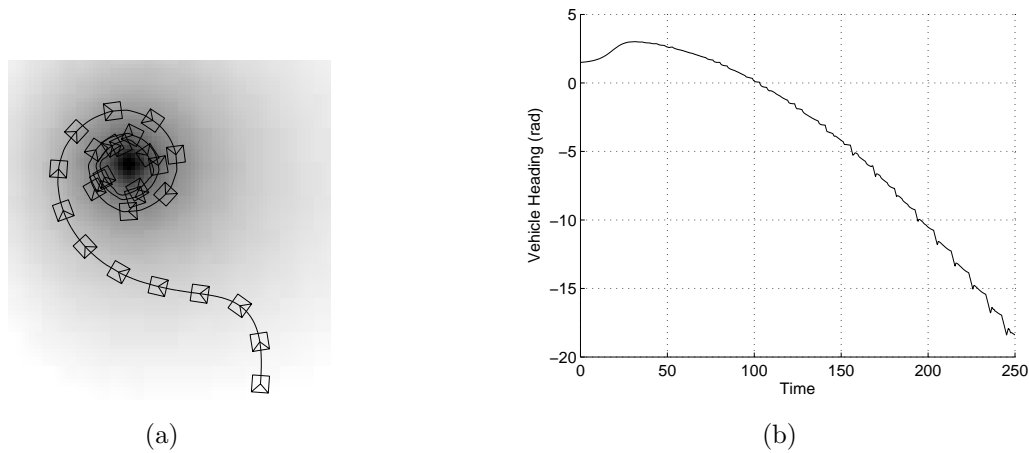
Figure 7: Simulations with a diffusion source

# 6   Proofs of Theorems 1 and 2

We examine the robot driven by the control law (3). Based on (7) and (12), we pick $\delta > 0$ and $\eta > 0$ such that

$$\delta < v_*, v \min_{\boldsymbol{r} \in W(a, \gamma_{\star\star})} \|\nabla D(\boldsymbol{r})\| - v_*, \tag{21}$$

$$\mu > \frac{v}{\delta} \max_{\boldsymbol{r} \in W(a,, \gamma_{\star\star}), |\alpha| \le \alpha(v_* + \delta, \boldsymbol{r})} |\varkappa(\alpha, \boldsymbol{r})| + \eta, \tag{22}$$

$$\mu > \frac{2v}{a\delta} \left( \left\lceil \frac{B(a)}{2\pi} \right\rceil + 1 \right) \tag{23}$$

Since these inequalities are strict, they, along with (5), remain true with $a + \varepsilon$ and $\gamma_{\star\star} + \varepsilon$ put in place of $a$ and $\gamma_{\star\star}$, respectively, for small enough $\varepsilon > 0$.

We observe that the closed-loop system (1), (3) is described by the following autonomous ordinary differential equations (ode) with respect to $\boldsymbol{r}, \theta$

$$\dot{\boldsymbol{r}} = v\vec{e}(\theta), \quad \dot{\theta} = \mu\big[\dot{d} - v_*\big], \quad \dot{d} = v\left\langle \nabla D(\boldsymbol{r}); \vec{e}(\theta) \right\rangle, \tag{24}$$

where $\langle \cdot; \cdot \rangle$ is the standard inner product For any state $(\boldsymbol{r}, \theta)$ of the system (24), we define $\sigma(\boldsymbol{r}, \theta) = \sigma$

$$\sigma := \begin{cases} 0 & \text{if } \nabla D(\boldsymbol{r}) \text{ and } \vec{e} \text{ are linearly dependent} \\ 1 & \text{if the angle from } \nabla D(\boldsymbol{r}) \text{ to } \vec{e} \text{ is positive} \\ -1 & \text{if the angle from } \nabla D(\boldsymbol{r}) \text{ to } \vec{e} \text{ is negative} \end{cases}$$

The first lemma displays the major feature of the control law (3) that ultimately ensures achievement of the objective.

**Lemma 1** *There exists $\omega > 0$ such that whenever $\boldsymbol{r} \in W(a + \varepsilon, \gamma_{\star\star} + \varepsilon)$, the following implications hold*

$$\dot{d} = v_* + \delta \Rightarrow \begin{cases} \ddot{d} \le -\omega & \text{if } \sigma = 1 \\ \ddot{d} \ge \omega & \text{if } \sigma = -1 \\ \ddot{d} \ge \omega & \text{if } \sigma = +1 \\ \ddot{d} \le -\omega & \text{if } \sigma = -1 \end{cases}. \tag{25}$$

*Proof* Whenever $|\dot{d} - v_*| = |v \langle \nabla D; \vec{e} \rangle - v_*| \le \delta$, a simple trigonometry shows that

$$\vec{e} = \|\nabla D(\boldsymbol{r})\|^{-1} \Phi_{\sigma\left(\frac{\pi}{2} - \alpha\right)} \nabla D(\boldsymbol{r}),$$

where

$$|\alpha| \le \alpha(v_* + \delta, \boldsymbol{r}) \tag{26}$$

and $\alpha(\delta, \boldsymbol{r})$ is given by (13). Hence due to (24), we have

$$\ddot{d} = v \left\langle \nabla D(\boldsymbol{r}); \dot{\vec{e}} \right\rangle + v \langle D''(\boldsymbol{r})\dot{r}; \vec{e} \rangle$$

$$\overset{(1)}{=} v\dot{\theta} \left\langle \nabla D(\boldsymbol{r}); \Phi_{\frac{\pi}{2}} \vec{e} \right\rangle + v^2 \langle D''(\boldsymbol{r})\vec{e}; \vec{e} \rangle \tag{27}$$

$$= v\dot{\theta} \frac{\left\langle \nabla D(\boldsymbol{r}); \Phi_{\frac{\pi}{2} + \sigma\left(\frac{\pi}{2} - \alpha\right)} \nabla D(\boldsymbol{r}) \right\rangle}{\|\nabla D(\boldsymbol{r})\|}$$

$$+ v^2 \frac{\left\langle D''(\boldsymbol{r})\Phi_{\sigma\left(\frac{\pi}{2} - \alpha\right)} \nabla D(\boldsymbol{r}); \Phi_{\sigma\left(\frac{\pi}{2} - \alpha\right)} \nabla D(\boldsymbol{r}) \right\rangle}{\|\nabla D(\boldsymbol{r})\|^2}$$

$$= v^2 \frac{\langle \nabla D(\boldsymbol{r}); \Phi_{-\sigma\alpha} \nabla D(\boldsymbol{r}) \rangle}{\|\nabla D(\boldsymbol{r})\|} \left\{ -\sigma \frac{\dot{\theta}}{v} \right.$$

$$\left. + \frac{\left\langle D''(\boldsymbol{r})\Phi_{\frac{\pi}{2} - \sigma\alpha} \nabla D(\boldsymbol{r}); \Phi_{\frac{\pi}{2} - \sigma\alpha} \nabla D(\boldsymbol{r}) \right\rangle}{\|\nabla D(\boldsymbol{r})\| \langle \nabla D(\boldsymbol{r}); \Phi_{-\sigma\alpha} \nabla D(\boldsymbol{r}) \rangle} \right\}$$

$$\overset{(8)}{=} \sigma v^2 \cos\alpha \|\nabla D(\boldsymbol{r})\| \left\{ -\frac{\dot{\theta}}{v} + \sigma \varkappa(\sigma\alpha, \boldsymbol{r}) \right\}; \tag{28}$$

$$v^2 \cos\alpha \|\nabla D(\boldsymbol{r})\| \overset{(26)}{\ge} v\sqrt{v^2 \|\nabla D(\boldsymbol{r})\|^2 - (v_* + \delta)^2}$$

$$\ge \xi := v\sqrt{v^2 \min_{\boldsymbol{r} \in W(a+\varepsilon)} \|\nabla D(\boldsymbol{r})\|^2 - (v_* + \delta)^2} \overset{(21)}{>} 0.$$

Whenever $\dot{d} = v_* + \delta$, (24) implies that

$$-\frac{\dot{\theta}}{v} + \sigma \varkappa_\sigma(\alpha, \boldsymbol{r}) = -\frac{\mu(\dot{d} - v_*)}{v} + \sigma \varkappa_\sigma(\alpha, \boldsymbol{r})$$

$$\leq -\frac{\mu\delta}{v} + |\varkappa_\sigma(\alpha, \boldsymbol{r})| \overset{(22)}{\leq} -\frac{\mu\delta}{v} + \frac{\delta(\mu - \eta)}{v} = -\frac{\delta\eta}{v} < 0.$$

Similarly whenever $\dot{d} = v_* + \delta$,

$$-\frac{\dot{\theta}}{v} + \sigma \varkappa_\sigma(\alpha, \boldsymbol{r}) \geq \frac{\mu\delta}{v} - |\varkappa_\sigma(\alpha, \boldsymbol{r})|$$

$$\overset{(22)}{\geq} \frac{\mu\delta}{v} - \frac{\delta(\mu - \eta)}{v} = \frac{\delta\eta}{v} > 0.$$

These inequalities complete the proof. $\quad\square$

**Lemma 2** *Suppose that $\dot{d} \leq v_* - \delta$ during a time interval $\Delta = [t_0, t_1]$. For $t \in \Delta$, the direction vector $\vec{e}(\theta)$ rotates clockwise with the angular velocity $\dot{\theta} \leq -\mu\delta$. The space deviation from the initial location and the total turning angle $\varphi := |\theta(t) - \theta(t_0)|$ obey the inequality*

$$\|\boldsymbol{r}(t) - \boldsymbol{r}(t_0)\| \leq q(\varphi) := \frac{2v}{\mu\delta} \left\lfloor \frac{\varphi}{2\pi} \right\rfloor + \frac{v}{\mu\delta} [1 - \cos\min\{\lfloor\varphi\rceil; \pi\}] \qquad (29)$$

*where $\lfloor \cdot \rfloor$ is the integer floor and $\lfloor\varphi\rceil := \varphi - 2\pi \left\lfloor \frac{\varphi}{2\pi} \right\rfloor$.*

*Proof* Without any loss of generality, it can be assumed that $\boldsymbol{r}(t_0) = 0, \theta(t_0) = 0$. The first claim of the lemma is immediate from the second equation in (24):

$$\dot{\theta} \overset{(24)}{=} \mu\left[\dot{d} - v_*\right] \overset{\dot{d} \leq v_* - \delta}{\leq} -\mu\delta.$$

So $s := -\theta$ can be taken as a new independent variable:

$$\frac{d\boldsymbol{r}}{ds} = u\vec{e}(-s), \quad u := -\frac{v}{\dot{\theta}} \in \left[0, \frac{v}{\mu\delta}\right].$$

The squared distance $\|\boldsymbol{r}(\varphi)\|^2$ does not exceed the maximal value of $I$ in the following optimization problem:

$$I := \|\boldsymbol{r}(\varphi)\|^2 \to \max \text{ subject to}$$

$$\frac{d\boldsymbol{r}}{ds} = u\vec{e}(-s) \ s \in [0, \varphi], \quad \boldsymbol{r}(0) = 0, \quad u(s) \in \left[0, \frac{v}{\mu\delta}\right].$$

By [34], its solution $\boldsymbol{r}^0(\cdot), u^0(\cdot)$ exists and satisfies the Pontryagin's maximum principle: there exists a differentiable function $\psi(s) \in \mathbb{R}^2$ such that

$$\frac{d\psi}{ds} = -\frac{\partial}{\partial \boldsymbol{r}} u^0 \psi^\top \vec{e}(-s) = 0 \Rightarrow \psi = \text{const},$$

$$\psi = \psi(\varphi) = -2\boldsymbol{r}^0(\varphi),$$

$$u^0(s) = \arg \max_{u \in [0, v/(\mu\delta)]} u\psi^\top \vec{e}(-s)$$

$$= \begin{cases} v/(\mu\delta) & \text{if } \psi^\top \vec{e}(-s) > 0 \\ 0 & \text{if } \psi^\top \vec{e}(-s) < 0 \,. \\ \text{unclear} & \text{if } \psi^\top \vec{e}(-s) = 0 \end{cases}$$

If $\boldsymbol{r}^0(\varphi) = 0$, (29) is evident. Let $\boldsymbol{r}^0(\varphi) \neq 0$. Then $\psi \neq 0$ and so as $s$ progresses, the function $u^0(\cdot)$ interchanges the values $0$ and $v/(\mu\delta)$, each taken on an interval of length $\pi$ possibly except for the extreme intervals whose lengths do not exceed $\pi$. Inequality (29) is straightforward from direct computation of $\|\boldsymbol{r}(\varphi)\|$ for such controls $u(\cdot)$, along with picking the maximum among these results. □

**Lemma 3** *Let the robot start at $t = t_0$ with $\dot{d} \leq v_* - \delta$ either from the isoline $I(\gamma_{\star\star})$ or from $\boldsymbol{r}_{\mathrm{in}}$, in which case $D(\boldsymbol{r}_{\mathrm{in}}) \leq \gamma_{\star\star}$. Then there exists a time $t_* \geq t_0$ such that $\dot{d}(t_*) = v_* - \delta, \ddot{d}(t_*) \geq 0, \|\boldsymbol{r}(t) - \boldsymbol{r}(t_0)\| \leq a \,\forall t \in [t_0, t_*]$.*

*Proof* For $k := \left\lceil \frac{B(a)}{2\pi} \right\rceil, \varphi := 2\pi(k + 1) > 0$, we have

$$\varphi = 2\pi \left( \left\lceil \frac{B(a)}{2\pi} \right\rceil + 1 \right) \geq B(a) + 2\pi, \tag{30}$$

$$q(\varphi) \overset{(29)}{=\!=} \frac{2v}{\mu\delta}(k + 1) \overset{(23)}{<} a. \tag{31}$$

If $\dot{d}(t_0) = v_* - \delta, \ddot{d}(t_0) \geq 0$, the claim is clear. Otherwise either $\dot{d}(t_0) < v_* - \delta$ or $\dot{d}(t_0) = v_* - \delta, \ddot{d}(t_0) < 0$; in both cases, the open set $S := \{t > t_0 : \dot{d}(t) < v_* - \delta\}$ contains all $t > t_0$ that are close enough to $t_0$. For the leftmost connected component $(0, t_*)$ of the intersection $S \cap \{t > t_0 : |\theta(t) - \theta(t_0)| < \varphi\}$, evidently either 1) $|\theta(t_*) - \theta(t_0)| = \varphi, \dot{d}(t_*) < v_* - \delta$ or 2) $\dot{d}(t_*) = v_* - \delta$. For $t \in [t_0, t_*]$, the robot remains in the disk $\mathfrak{D} := \{\boldsymbol{r} : \|\boldsymbol{r} - \boldsymbol{r}(t_0)\| \leq a\}$ due to (29) and (31). This disk does not contain $\boldsymbol{r}^0$ thanks to (5).

    1) As $t$ runs from $t_0$ to $t_*$, the gradient $\nabla D[\boldsymbol{r}(t)]$ turns through an angle that does not exceed $B(a)$ due to (11). Meanwhile, $\vec{e}(\theta)$ turns clockwise through

the angle $\varphi$. By (30) and the continuity argument, $\nabla D[\boldsymbol{r}(t)]$ and $\vec{e}[\theta(\tau)]$ are identically directed at some time instant $\tau \in [0, t_*]$. Then

$$\dot{d}(\tau) = v \langle \nabla D[\boldsymbol{r}(\tau)]; \vec{e}[\theta(\tau)] \rangle = v \, \|\nabla D[\boldsymbol{r}(\tau)]\| \overset{(7)}{>} v_*,$$

which is impossible since $\dot{d}(t) \leq v_* - \delta \; \forall t \in [0, t_*] \subset \overline{S}$. Hence case 1) does not occur.

2) The proof is completed by noting that $\dot{d}(t) < v_* - \delta \; \forall t \in (0, t_*) \wedge \dot{d}(t_*) = v_* - \delta \Rightarrow \ddot{d}(t_*) \geq 0$. $\quad\square$

**Lemma 4** *In a finite time, the robot reaches the set $V_{\star\star} := \{\boldsymbol{r} : D(\boldsymbol{r}) > \gamma_{\star\star}\}$ bounded by the isoline $I(\gamma_{\star\star})$.*

*Proof* Suppose to the contrary that the claim is incorrect

$$\boldsymbol{r}_{\text{in}} \notin V_{\star\star} \Leftrightarrow D(\boldsymbol{r}_{\text{in}}) \leq \gamma_{\star\star} \qquad \forall t \geq 0 \tag{32}$$

and consider separately several cases.

**(a)** $v_* - \delta \leq \dot{d}(0) \leq v_* + \delta, \sigma(0) = 1$. By (25), $L := \{t \geq 0 : \boldsymbol{r}(t) \text{ lies in the interior of } W(a + \varepsilon, \gamma_{\star\star} + \varepsilon)\}$ and $M := \{t > 0 : v_* - \delta < \dot{d}(t) < v_* + \delta\}$ contain all small enough $t > 0$. Let $(0, t_*)$ be the leftmost connected component of $L \cap M$. Since $0 < v_* - \delta < \dot{d}(t) \; \forall t \in (0, t_*)$, (32) implies that $t_* < \infty$. So (6) entails that either 1) $\dot{d}(t_*) = v_* \pm \delta$ or 2) $D[\boldsymbol{r}(t_*)] = \gamma_{\star\star} + \varepsilon$ (since $d(t)$ ascends while $t \in (0, t_*)$). However 2) does not hold by (32). As $t$ runs from 0 to $t_*$ in the case 1),

$$|\langle \nabla D[\boldsymbol{r}(t)]; \vec{e}[\theta(t)] \rangle| = \frac{|\dot{d}(t)|}{v} \leq \frac{v_* + \delta}{v} \overset{(21)}{<} \|\nabla D[\boldsymbol{r}(t)]\|.$$

So $\nabla D[\boldsymbol{r}(t)]$ and $\vec{e}[\theta(t)]$ are not co-linear and hence $\sigma$ does not change its value 1. Hence $\dot{d}(t)$ cannot arrive at the values $v_* \pm \delta$ by (25). Thus we have arrived at a contradiction.

**(b)** $\dot{d}(0) \leq v_* - \delta$. By Lemma 3 (with $t_0 := 0$), there exists a time $t_* \geq t_0$ such that $\|\boldsymbol{r}(t) - \boldsymbol{r}(t_0)\| \leq a$ and so by (6), $\boldsymbol{r}(t) \in W(a, \gamma_{\star\star})$ for all $t \in [t_0, t_*]$, and $\dot{d}(t_*) = v_* - \delta, \ddot{d}(t_*) \geq 0$. Then $\sigma(t_*) = 1$ by (25), and retracing the arguments from (a) still results in a contradiction.

**(c)** $\dot{d}(0) > v_* - \delta$. Let $[0, t_*)$ be the leftmost connected component of $\{t \geq 0 : \dot{d}(t) > v_* - \delta\}$. Since $v_* > \delta$ by (21), $t_* < \infty$ due to (32) and $D[\boldsymbol{r}(t)] \geq D[\boldsymbol{r}_{\text{in}}] \; \forall t \in [0, t_*]$. By retracing the arguments from (b) (with $t_0 : +t_*$), we arrive at a contradiction once more.

The contradictions obtained prove that (32) does not hold, which completes the proof. $\square$

**Lemma 5** *The robot cannot leave the desired vicinity* (2) *of the maximizer from any location in $V_{\star\star}$.*

*Proof* Suppose to the contrary that the robot leaves $V_\star$ from some location $\boldsymbol{r}(0) \in V_{\star\star}$. Here $D[\boldsymbol{r}(0)] > \gamma_{\star\star}$ by the definition of $V_{\star\star}$ from Lemma 4, and due to (4), (5), the robot necessarily intersects the isolines $I(\gamma_*)$ and $I(\gamma_{\star\star})$, where $I(\gamma) = \{\boldsymbol{r} : D(\boldsymbol{r}) = \gamma\}$. Let $t_1 > 0$ be the earliest time $t$ such that $D[\boldsymbol{r}(t)] = \gamma_\star$, and let $t_0$ be the latest time $t \in (0, t_1)$ such that $D[\boldsymbol{r}(t)] = \gamma_{\star\star}$. Then $D[\boldsymbol{r}(t)] < \gamma_{\star\star} \; \forall t \in (t_0, t_1)$ and so $\dot{d}(t_0) \leq 0 < v_* - \delta$. By Lemma 3, there exists a time $t_* \geq t_0$ such that $\dot{d}(t_*) = v_* - \delta, \ddot{d}(t_*) \geq 0, \|\boldsymbol{r}(t) - \boldsymbol{r}(t_0)\| \leq a \; \forall t \in [t_0, t_*]$. The last relation and (5) imply that the robot does not reach the isoline $I(\gamma_\star)$ for $t \in [t_0, t_*]$ and so $\gamma_\star < D[\boldsymbol{r}(t)] \leq \gamma_{\star\star} \; t \in [t_0, t_*]$. By (6), this yields that $\boldsymbol{r}(t_*) \in W(a + \varepsilon, \gamma_{\star\star} + \varepsilon)$. Then $\dot{d}(t_*) = v_* - \delta, \ddot{d}(t_*) \geq 0$ imply that $\sigma(t_*) = 1$ thanks to (25). By retracing the arguments from (a) in the proof of Lemma 4, we conclude that since $t_*$ and until the robot enters $V_{\star\star}$ once more, $d(t)$ ascends. So $D[\boldsymbol{r}(t)], t \geq t_0$ cannot reach the value $\gamma_\star$ earlier than it reaches $\gamma_{\star\star}$ for the second time, in violation of the definitions of $t_0, t_1$. The contradiction obtained proves the lemma. $\square$

**PROOF OF THEOREM 2:** This theorem is immediate from Lemmas 4 and 5. $\square$

**PROOF OF THEOREM 1:** This theorem is immediate from Theorem 2 and Remark 3. $\square$

# References

[1] K. Ahnert and M. Abel. Numerical differentiation of experimental data: local versus global methods. *Computer Physics Communications*, 177:764774, 2007.

[2] M.E. Alpay and M.H. Shor. Model-based solution techniques for the source localization problem. *IEEE Transactions on Control Systems Technology*, 8(6):895–904, 2000.

[3] K.B. Ariyur and M. Krstic. *Real-Time Optimization by Extremum-Seeking Feedback.* Wiley-Interscience, Hoboken, NJ, 2003.

[4] R. Bachmayer and N.E. Leonard. Vehicle networks for gradient descent in a sampled environment. In *Proceedings of the 41st IEEE Conf. on Decision and Control*, pages 113–117, Las Vegas, NV, December 2002.

[5] D. Baronov and J. Baillieul. Autonomous vehicle control for ascending/descending along a potential field with two applications. In *Proceedings of the American Control Conference*, pages 678–683, Seattle, WA, June 2008.

[6] F. B. Belgacem. Identifiability for the pointwise source detection in Fisher's reaction–diffusion equation. *Inverse Problems*, 28(6), 2012.

[7] E. Biyik and M. Arcak. Gradient climbing in formation via extremum seeking and passivity-based coordination rules. In *Proceedings of the 46th IEEE Conf. on Decision and Control*, pages 3133–3138, New Orleans, LA, December 2007.

[8] E. Burian, D. Yoeger, A. Bradley, and H. Singh. Gradient search with autonomous underwater vehicle using scalar measurements. In *Proceedings of the IEEE Symposium on Underwater Vehicle Technology*, pages 86–98, Monterey, CA, June 1996.

[9] A. G. Butkovskiy and L. M. Pustyl'nikov. *Mobile Control of Distributed Parameter Systems*. Halsted Press, NY, 1987.

[10] R. Chartrand. Numerical differentiation of noisy nonsmooth data. *ISRN Appl. Math.*, 2011. doi: 10.5402/2011/164564.

[11] V. Christopoulos and S. I. Roumeliotis. Multirobot trajectory generation for single source explosion parameter estimation. In *Proceedings of the 2005 IEEE Int. Conf. on Robotics and Automation*, pages 2814–2820, Barcelona, Spain, April 2005.

[12] J. Cochran and M. Krstic. Nonholonomic source seeking with tuning of angular velocity. *IEEE Trans. Autom. Control*, 54:717–731, 2009.

[13] J. Cortes. Distributed gradient ascent of random fields by robotic sensor networks. In *Proceedings of the 46th IEEE Conference on Decision and Control*, pages 3120–3126, New Orleans, LA, December 2007.

[14] M.A. Demetriou. Power management of sensor networks for detection of a moving source in 2-D spatial domains. In *Proceedings of the American Control Conference*, pages 1144–1149, Minneapolis, MN, June 2006.

[15] M.A. Demetriou. Process estimation and moving source detection in 2-D diffusion processes by scheduling of sensor networks. In *Proceedings of the American Control Conference*, New York, NY, July 2007.

[16] M.A. Demetriou. Centralized and decentralized policies for the containment of moving source in 2-D diffusion processes using sensor/actuator network. In *Proceedings of the American Control Conference*, pages 127–132, St. Louis, MO, June 2009.

[17] Y. Elor and A. M. Bruckstein. Two-robot source seeking with point measurements. *Theoretical Computer Sciences*, 457:76–85, 2012.

[18] V. Gazi and K. M. Passino. Stability analysis of social foraging swarms. *IEEE Trans. on Systems, Man, and Cybernetics*, 54(1):539–557, 2004.

[19] A. Gray. Logarithmic spirals. In *Modern Differential Geometry of Curves and Surfaces with Mathematica*, pages 40–42. CRC Press, Boca Raton, second edition, 1997.

[20] R. Horst and P. M. Pardalos (eds.). *Handbook of Global Optimization*. Kluwer Academic Publishers, Dordrecht, 1995.

[21] W. Jatmiko, F. Jovan, R. Dhiemas, A. M. Sakti, F. M. Ivan, T. Fukuda, and K. Sekiyama. Robots implementation for odor source localization using PSO algorithm. *WSEAS Transactions on Circuits and Systems*, 10(4):115–125, 2011.

[22] A. Khapalov. Source localization and sensor placement in environmental monitoring. *International Journal of Applied Mathematics and Computer Science*, 20(3):445–458, 2010.

[23] H. Lee, V.I. Utkin, and A. Malinin. Chattering reduction using multiphase sliding mode control. *International Journal of Control*, 82:1720 – 1737, 2009.

[24] W. Li, J. A. Farrell, Sh. Pang, and R. M. Arrieta. Moth-inspired chemical plume tracing on an autonomous underwater vehicle. *IEEE Transactions on Robotics*, 22(2):292–307, 2006.

[25] S. Liu and M. Krstic. Stochastic source seeking for nonholonomic unicycle. *Automatica*, 48(9):1443–1453, 2010.

[26] A. S. Matveev, H. Teimoori, and A. V. Savkin. Navigation of a unicycle-like mobile robot for environmental extremum seeking. *Automatica*, 47(1):85–91, 2011.

[27] A. Mesquita, J. Hespanha, and K. Åström. Optimotaxis: a stochastic multi-agent optimization procedure with point measurements. In M. Egersted and B. Mishra, editors, *Hybrid Systems: Computation and Control*, volume 4981, pages 358–371. Springer-Verlag, Berlin, 2008.

[28] P. Ögren, E. Fiorelli, and N. E. Leonard. Cooperative control of mobile sensor networks: Adaptive gradient climbing in a distributed environment. *IEEE Trans. Autom. Control*, 49(8):1292–1301, 2004.

[29] B. Porat and A. Neohorai. Localizing vapor-emitting sources by moving sensors. *IEEE Trans. Signal Processing*, 44(4):1018–1021, 1996.

[30] P. Pyk, S. Badia, U. Bernardet, P. Knsel, M. Carlsson, J. Gu, E. Chanie, B. Hansson, T. Pearce, and P. Verschure. An artificial moth: Chemical source localization using a robot based neuronal model of moth optomotor anemotactic search. *Autonomous Robots*, 20(3):197–213, 2006.

[31] I. F. Sivergina, M. P. Polis, and I. Kolmanovsky. Source identification for parabolic equations. *Mathematics of Control, Signals, and Systems*, 16(16):141–157, 2003.

[32] P. Tzanos and M. Žefran. Locating a circular biochemical source: Modeling and control. In *Proceedings of the 2007 IEEE Int. Conf. on Robotics and Automation*, pages 523–528, Rome, Italy, 2007.

[33] L. K. Vasiljevic and H. K. Khalil. Error bounds in differentiation of noisy signals by high-gain observers. *Systems & Control Letters*, 57:856–862, 2008.

[34] R. B. Vinter. *Optimal Control*. Birkhäuzer, Boston, 2000.

[35] C. Zhang, D. Arnold, N. Ghods, A. Siranosian, and M. Krstic. Source seeking with non-holonomic unicycle without position measurement and with tuning of forward velocity. *Systems & Control Letters*, 56:245–252, 2007.

# A   Proof of Remark 2

$$\nabla D = \rho \vec{e}(\varphi) \Rightarrow \begin{matrix} D'_x = \rho \cos \varphi \\ D'_y = \rho \sin \varphi \end{matrix} \Rightarrow D'' =$$

$$= \begin{pmatrix} \rho'_x \cos \varphi - \rho \varphi'_x \sin \varphi & \rho'_y \cos \varphi - \rho \varphi'_y \sin \varphi \\ \rho'_x \sin \varphi + \rho \varphi'_x \cos \varphi & \rho'_y \sin \varphi + \rho \varphi'_y \cos \varphi \end{pmatrix}$$

$$= \vec{e}(\varphi) \left( \nabla \rho \right)^\top + \rho \Phi_{\frac{\pi}{2}} \vec{e}(\varphi) \left( \nabla \varphi \right)^\top ; \tag{33}$$

$$D''_{xy} = D''_{yx} \Rightarrow \left\langle \nabla \rho ; \Phi_{\frac{\pi}{2}} \vec{e}(\varphi) \right\rangle = \rho \left\langle \nabla \varphi ; \vec{e}(\varphi) \right\rangle ; \tag{34}$$

$$\varkappa(\alpha, \boldsymbol{r}) \overset{(8)}{=\!=} \frac{\left\langle D''(\boldsymbol{r}) \Phi_{\frac{\pi}{2}-\alpha} \vec{e}(\varphi) ; \Phi_{\frac{\pi}{2}-\alpha} \vec{e}(\varphi) \right\rangle}{\rho \cos \alpha}$$

$$\overset{(33)}{=\!=} \frac{\left\langle \nabla \rho ; \Phi_{\frac{\pi}{2}-\alpha} \vec{e}(\varphi) \right\rangle \left\langle \vec{e}(\varphi) ; \Phi_{\frac{\pi}{2}-\alpha} \vec{e}(\varphi) \right\rangle}{\rho \cos \alpha}$$

$$+ \frac{\rho \left\langle \nabla \varphi ; \Phi_{\frac{\pi}{2}-\alpha} \vec{e}(\varphi) \right\rangle \left\langle \Phi_{\frac{\pi}{2}} \vec{e}(\varphi) ; \Phi_{\frac{\pi}{2}-\alpha} \vec{e}(\varphi) \right\rangle}{\rho \cos \alpha}$$

$$= \frac{\tan \alpha}{\rho} \left\langle \nabla \rho ; \Phi_{\frac{\pi}{2}-\alpha} \vec{e}(\varphi) \right\rangle + \left\langle \nabla \varphi ; \Phi_{\frac{\pi}{2}-\alpha} \vec{e}(\varphi) \right\rangle ;$$

$$\left\langle \nabla \rho ; \Phi_{\frac{\pi}{2}-\alpha} \vec{e}(\varphi) \right\rangle = \left\langle \nabla \rho ; \Phi_{\frac{\pi}{2}} \vec{e}(\varphi) \right\rangle$$

$$+ \left\langle \nabla \rho ; \left[ \Phi_{\frac{\pi}{2}-\alpha} - \Phi_{\frac{\pi}{2}} \right] \vec{e}(\varphi) \right\rangle \overset{(34)}{=\!=} \rho \left\langle \nabla \varphi ; \vec{e}(\varphi) \right\rangle$$

$$+ 2 \sin \frac{\alpha}{2} \left\langle \nabla \rho ; \Phi_{-\frac{\alpha}{2}} \vec{e}(\varphi) \right\rangle .$$

Summarizing, we arrive at (10).